ARTICLE

Evidence for Singlet-Oxygen Generation and Biocidal Activity in Photoresponsive Metallic Nitride Fullerene–Polymer Adhesive Films

D. Michelle McCluskey,[†] Tiffany N. Smith,[†] Praveen K. Madasu,[†] Curtis E. Coumbe,[†] Mary A. Mackey,[†] Preston A. Fulmer,[‡] James H. Wynne,[‡] Steven Stevenson,[†] and J. Paige Phillips*[,†]

Department of Chemistry and Biochemistry, University of Southern Mississippi, Hattiesburg, Mississippi 39406, and Chemistry Division, Naval Research Laboratory, Washington, D.C. 20375

ABSTRACT The adhesive properties, as measured by bulk tack analysis, are found to decrease in blends of isomerically pure $Sc_3N@I_h$-C_{80} metallic nitride fullerene (MNF) and polystyrene-*block*-polyisoprene-*block*-polystyrene (SIS) copolymer pressure-sensitive adhesive under white light irradiation in air. The reduction of tack is attributed to the in situ generation of $^1O_2$ and subsequent photooxidative cross-linking of the adhesive film. Comparisons are drawn to classical fullerenes C_{60} and C_{70} for this process. This work represents the first demonstration of $^1O_2$ generating ability in the general class of MNFs ($M_3N@C_{80}$). Additional support is provided for the sensitizing ability of $Sc_3N@I_h$-C_{80} through the successful photooxygenation of 2-methyl-2-butene to its allylic hydroperoxides in benzene-d_6 under irradiation at 420 nm, a process that occurs at a rate comparable to that of C_{60}. Photooxygenation of 2-methyl-2-butene is found to be influenced by the fullerene sensitizer concentration and O_2 flow rate. Molar extinction coefficients are reported for $Sc_3N@I_h$-C_{80} at 420 and 536 nm. Evaluation of the potential antimicrobial activity of films prepared in this study stemming from the in situ generation of $^1O_2$ led to an observed 1 log kill for select Gram-positive and Gram-negative bacteria.

KEYWORDS: singlet oxygen • polymer film • PSA • metallic nitride fullerene • adhesive • fullerene • metallofullerene • MNF • $Sc_3N@C_{80}$ • antimicrobial • biocidal

1. INTRODUCTION

The photophysical properties of empty-cage fullerenes (e.g., C_{60} and C_{70}), their ability to generate singlet oxygen, and their potential impact on medical applications have been well-documented (1–14). This phenomenon is not limited to classical empty-cage structures, as several other types of fullerenes have emerged recently with the capacity to sensitize the formation of singlet oxygen. In 2001, members of the azafullerene fullerene family, e.g., $(C_{59}N)_2$ and $C_{59}NH$, joined classical empty-cage fullerenes in reports of singlet-oxygen formation (15, 16) but with about half the efficiency of C_{60}. In the same year, several classical endohedral metallofullerenes (EMFs), e.g., $Dy@C_{82}$ and $Gd@C_{82}$, were also shown to generate singlet oxygen and efficiently sensitize the photooxidation of olefins in an ene reaction (17). Often this ene reaction is used as a diagnostic tool for the generation of singlet oxygen, where the detection of photooxygenated products is attributed to the singlet-oxygen-mediated process (18–21). EMFs have generated a great deal of excitement over their empty-cage cousins because the inclusion of a metal or metals within the fullerene cage offers increased potential resulting from the unique properties of the encapsulated metal. Possible applications under development include their use in optoelectronic devices and energy conversion systems (17). Metallic nitride fullerenes (MNFs), e.g. $Sc_3N@C_{80}$ and $Gd_3N@C_{80}$, represent an even more recent addition to the metallofullerene class of compounds and are characterized by the incorporation of a metal–nitride complex, M_3N, inside an all-carbon C_{80} cage. Although there have been no literature reports of singlet-oxygen generation from this class of compounds, other application areas that are discussed include their use as magnetic resonance imaging (MRI) contrast agents (22, 23) and in photovoltaic devices (24).

A consequence of the ability of C_{60} to generate singlet oxygen is the development of new application areas such as fullerene-based, antimicrobial agents. Kai et al. (8) have demonstrated the antibacterial activity of C_{60} dissolved with poly(vinylpyrrolidone) K30. Fang et al. (25) have shown the effect of C_{60} on both Gram-negative and Gram-positive bacteria in terms of their phospholipid composition. Lyon et al. (26–28) have described the antibacterial activity of fullerene–water suspensions, and Li et al. (29) provide an overview of antimicrobial nanomaterials such as C_{60} for water disinfection and microbial control. One of the central technical efforts of our fullerene–polymer research has been the study of how to incorporate metallofullerene nanomaterials into macrostructures (e.g. dendrimers, polymers, films, and devices) and exploit their benefits as multifunc-

* To whom correspondence should be addressed. Phone: (601) 266-4083. Fax: (601) 266-6075. E-mail: Janice.Phillips@usm.edu.

Received for review January 6, 2009 and accepted February 23, 2009

[†] University of Southern Mississippi.

[‡] Naval Research Laboratory.

DOI: 10.1021/am900008v

Published on Web 03/20/2009

tional and, in many cases, stimuli-responsive materials, for example, MRI active + antimicrobial.

Polymer blends and cross-linked networks containing fullerene nanomaterials may have potential for use in photovoltaic cells (30−32), nonlinear optical devices (33−36), and as oxygen sensors (37). Our group's research interests lie in discovering the unique properties of polymer nanocomposite structures containing fullerene-based nanomaterials. In this effort, we recently reported the chemical, mechanical, and adhesive properties of interesting stimuli-responsive nanocomposites prepared from rubber-based, pressure-sensitive adhesive (PSA)−C_{60} fullerene blends (38, 39). PSAs are widely utilized in commercial tape, label manufacturing, and medical adhesives and may be produced to have a variety of chemical compositions, such as acrylic, silicone, and rubber-based systems (40). Rubber-based systems are typically highly flexible and elastic, and the polystyrene-*block*-polyisoprene-*block*-polystyrene (SIS) copolymer is an example of a commonly applied thermoplastic elastomer-based PSA (41). These block copolymers have high cohesive strength because of the physical cross-linking, which results from the microphase separation of the hard, high-T_g, polystyrene segments from the rubbery portions derived from the unsaturated polyisoprene center blocks (42).

Our group has demonstrated that the adhesive properties of rubber-based elastomeric adhesives, such as SIS, can be dramatically affected when blended with common photochemical sensitizers for the formation of singlet oxygen, including rose bengal, acridine, and C_{60} fullerene (38, 39). The photochemical efficiency of a photosensitizer to generate singlet oxygen is the singlet-oxygen quantum yield, Φ_Δ, and is reported to be high (0.8−1) for acridine, rose bengal, and C_{60} fullerene in common solvents at visible wavelengths (3−7, 21). Solubility variations, knowledge of singlet-oxygen quantum yields, and wavelength-dependent absorption extinction coefficients as solid film constituents limited detailed direct comparisons; however, C_{60} fullerene was consistently the superior singlet-oxygen generator as measured by a subsequent loss in adhesion of our nanocomposite systems. Purge gas experiments confirmed that the presence of oxygen was essential to the mechanism of adhesive loss, and in combination with the effects of added singlet-oxygen generators and scavengers, these results supported a singlet-oxygen-mediated process.

As part of our continuing interest in discovering the unique properties of polymer nanocomposites containing fullerene-based nanomaterials, we have extended this photochemical study to include isomerically purified $Sc_3N@I_h$-C_{80} (Figure 1) and evaluated its ability to produce singlet oxygen in solution and polymer films. This behavior, when extended to other MNF species, has the potential to produce a unique family of stimuli-responsive materials containing functional metals. These MNF−polymer nanocomposite films may hold promise for photovoltaic, photonic, electronic, and biomedical applications. With regard to specific applications, the films produced in this study were evaluated for potential antimicrobial activity resulting from the in situ generation of singlet oxygen.

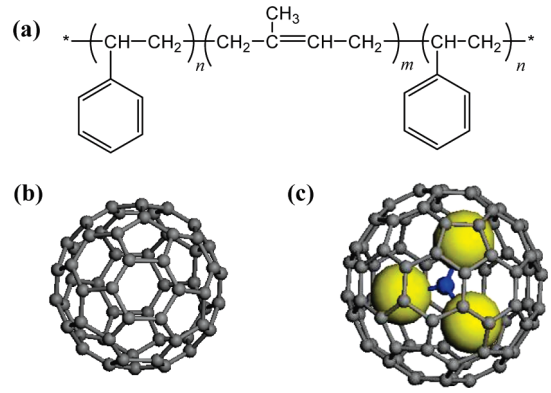

FIGURE 1. Chemical structures of (a) SIS copolymer PSA, (b) C_{60} fullerene, and (c) $Sc_3N@I_h$-C_{80} metallic nitride fullerene (Sc_3-MNF) sensitizer.

2. EXPERIMENTAL SECTION

Materials. Triblock polymer SIS (D1161) was provided by Kraton Polymers, Inc. (Belpre, OH) and was comprised of ~15 wt % polystyrene stabilized with 0.14 wt % Irganox 565 antioxidant. Gel permeation chromatography analysis yielded M_w fractions of 315 800 (64%) and 102 500 (36%) and polydispersities of 1.08 and 2.45. Toluene (>99.9% HPLC grade), benzene-d_6 (>99%), and 2-methyl-2-butene (>99.5%) were purchased from Sigma Aldrich (St Louis, MO). C_{60} and C_{70} were purchased from MER Corp. (Tucson, AZ). The production, separation, and isolation of isomerically pure (>99%) $Sc_3N@I_h$-C_{80} used in this study were performed by our new, nonchromatographic purification method as previously described (43, 44). Unless otherwise indicated, all materials were used as received without further purification.

Photochemical Studies: Solution. Solutions for photochemical studies were prepared by the addition of a catalytic amount of the fullerene sensitizer, C_{60} or $Sc_3N@I_h$-C_{80}, to a benzene-d_6 solvent with brief sonication to dissolve solids. 2-Methyl-2-butene was added to the sensitizer solution, which was then transferred to a 250 mL, borosilicate-glass-jacketed photochemical reaction vessel (Ace Glass Inc.). Irradiation was conducted using a Rayonet photochemical reactor fitted with seven, 420 nm λ_{max} bulbs. The reaction temperature was maintained at 15 °C by use of a circulating chiller, which was connected to the jacketed portion of the reaction vessel. The system was purged at a constant rate with dry O_2 for 30 min prior to the initiation of exposure and maintained for the duration of the reaction. Aliquots of approximately 0.7 mL were removed from the reaction vessel via a syringe and analyzed immediately using a 300 MHz/52 MM Bruker NMR. Peroxide products were reduced in a 1 M triphenylphosphine solution for safe handling and disposal. Molar extinction coefficients were determined for fullerene sensitizers through Beer's law plots of a serially diluted 7.75×10^{-5} M C_{60} or $Sc_3N@I_h$-C_{80} starting solution followed by UV/vis analysis on a Shimadzu UV-2401PC spectrometer.

Photochemical Studies: Film Preparation and Bulk Tack Analysis. The SIS polymer was dissolved in a toluene solution containing C_{60} or C_{70} fullerene or $Sc_3N@I_h$-C_{80} MNF and stirred overnight in the dark to prevent early exposure to light. Using an eight-path wet film applicator (Paul N. Gardner Company, Inc., Pompano Beach, FL), bulk tack samples were drawn on Q-panel brand test panels from 20 wt % solid solutions in toluene, followed by solvent evaporation in a dark hood overnight. The prepared films averaged 25−30 μm thickness and were visually uniform. Unless otherwise indicated, film samples were irradiated using a 150 W tungsten/halogen white-light

source. The radiation intensity was measured at the sample (30 s at 22 °C) with a "power puck" photometer to give 0.004 W/cm^2 visible and no measurable UV-A, UV-B, or UV-C light.

Bulk tack studies were conducted on the TA.XTplus texture analyzer (Godelming, Surrey, U.K.). An applied force (35 g) on the 1 in. round probe tip (57R stainless steel) and a probe insertion speed of 0.1 mm/s gave an insertion depth of 10% film thickness. The applied force was held for 10 s, and then the probe tip was withdrawn at a constant rate of 0.1 mm/s. The applied mass required to remove the probe tip from the film was obtained in grams per unit time, and the highest point was recorded as the peak tack. The probe tip was cleaned with a toluene solvent and dried after each tack experiment.

Antimicrobial Studies. Sensitizer-containing polymer solutions were prepared as described above and flow-coated onto glass microscope slides, which were maintained in the dark until the bacterial challenge was conducted. These slides were prepared in triplicate at 0.2 and 1.0 wt % fullerene sensitizer. Control slides were prepared by similarly flow-coating a SIS polymer solution containing no fullerene sensitizer.

Bacteria and Media. Luria–Bertani (LB) media (Difco Laboratories, Detroit, MI) was used as a bacterial growth medium for the preparation of bacteria for bacterial challenges and was prepared according to manufacturer's specifications. *Staphylococcus aureus* (*ATCC 25923*) was used for all Gram-positive bacterial challenges, and *Escherichia coli* (*ATCC 25922*) was used for all Gram-negative bacterial challenges.

Bacterial Challenge. Overnight cultures were grown in LB media, pelleted, and resuspended in a 0.5% saline solution at a concentration of 10^9 CFU/mL. An aliquot of 20 uL (10^7 CFU) of the bacterial suspension was deposited as a liquid droplet using a calibrated pipette onto a 1 cm^2 area of each coating. The bacteria were exposed to white light under ambient conditions for 2 h. The coatings were then swabbed with a sterile cotton swab that had been dipped in LB broth to ensure bacteria recovery and then placed in 5 mL of LB broth. The broth was then serially diluted seven times. The dilution series were incubated at 37 °C for 18 h, after which tubes were visually examined and determined to have growth by the presence of turbidity. log kill was determined by the following relationship: log kill = 7 − highest dilution exhibiting bacterial growth.

3. RESULTS AND DISCUSSION

Film Photochemical Studies: Bulk Tack Analysis. Our group has found that the bulk tack measurement is capable of not only monitoring the gain or loss in adhesive properties but also providing mechanistic insight into the chemical species produced during irradiation. For example, as more polar species are produced, such as peroxides, an increase in tack is observed. Using Fourier transform infrared analysis, peak tacks can be correlated to the production of these reactive peroxide intermediates. A preferred molecular structure of a PSA could be generally described as a network having minimal cross-link density and a sufficiently low plateau modulus to yield a high compliance of the adhesive and a good contact with the surface. Extensive chemical cross-linking in the elastic segment results in an increase of the modulus above Dahlquist's criterion ~10^5 Pa. The photochemically altered polymer adhesive films therefore exhibit more glassy behavior, and tack is reduced.

Figure 2 illustrates the changes in the adhesive bulk tack as a function of the fullerene sensitizer identity and visible exposure time in fullerene–SIS composite adhesive films. Bulk tack of control films, prepared without sensitizer,

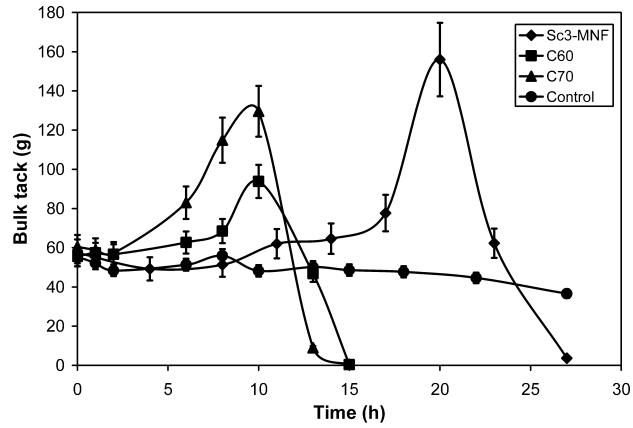

FIGURE 2. Change in the bulk tack of SIS films as a function of the fullerene sensitizer identity (e.g., C_{60}, C_{70}, or $Sc_3N@I_h$-C_{80}) and visible irradiation exposure time. Films are prepared containing equal concentrations, 2.0×10^{-4} mmol of sensitizer/g of polymer, and irradiated for 0–30 h using a 150 W tungsten/halogen light source in air. Each data point represents the average of the peak tack of five individual measurements.

remains relatively unchanged as a function of the exposure time, thus negating a significant thermal contribution to the tack measurement. The temperature of the test coupons increases approximately 20 °C over the first 30 min of irradiation, using a 150 W tungsten/halogen lamp at 6 in. distance from samples to source, and remains constant thereafter. Incorporation of as little as 2.0×10^{-4} mmol of sensitizer/g of polymer leads to dramatic effects on the tack/time adhesive plot. This low concentration of sensitizer—C_{60}, C_{70}, and $Sc_3N@I_h$-C_{80}—was employed to better discern any differences among the fullerene series and provide relative kinetic details. C_{60} and C_{70} fullerenes possess similar sensitizing ability when incorporated into SIS films, and the tack/time plot shows the now characteristic parabolic shape just prior to the complete loss of tack. This transient increase in tack has been attributed to the generation and subsequent decomposition of reactive peroxide intermediates during irradiation. When incorporated into SIS adhesive films, isomerically pure $Sc_3N@I_h$-C_{80} does lead to a loss in adhesive tack, however, at a reduced rate relative to C_{60} and C_{70} classical fullerenes. The shape of the $Sc_3N@I_h$-C_{80} tack/time plot is also characteristic of the singlet-oxygen-mediated process. Knowledge of singlet-oxygen quantum yields and wavelength-dependent absorption extinction coefficients as solid film constituents is required for direct comparisons; however, one can conclude that under these conditions $Sc_3N@I_h$-C_{80} is less able to productively generate singlet oxygen as measured by polymer–singlet oxygen chemical reactions, leading to the loss of adhesive tack.

Solution Photochemical Studies: Photooxygenation of 2-Methyl-2-butene. To provide further support for the ability of $Sc_3N@I_h$-C_{80} to photochemically generate singlet oxygen, solution studies were performed in a photochemical reactor under visible irradiation, using a modified procedure from that reported by Shinohara et al. (17). In this process, evidence for singlet-oxygen generation is detected by the successful photooxygenation of 2-methyl-2-butene to the allylic hydroperoxides shown

Scheme 1

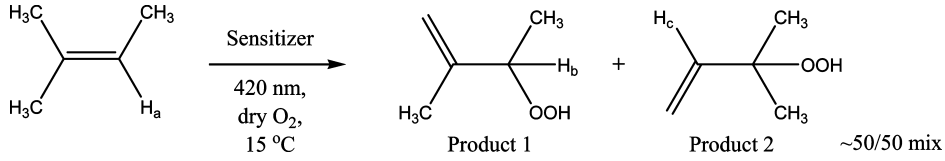

Table 1. Ene Photooxygenation of 2-Methyl-2-butene with Photogenerated Singlet Oxygen from Fullerene Sensitizers

sensitizer (C_{60} or Sc_3-MNF)	sensitizer concn (mM)	O_2 flow rate[a] (mL/min)	conversion[b] % P1 + % P2
none	none	120	0.0
C_{60}	0.045	120	15.6 (±1.0)
C_{60}	0.045	12	6.3 (±1.0)
C_{60}	0.0045	120	5.2 (±0.9)
Sc_3-MNF	0.045	120	12.4 (±0.6)
Sc_3-MNF	0.045	12	5.1 (±0.7)
Sc_3-MNF	0.0045	120	7.0 (±1.3)

[a] The O_2 flow rate is adjusted using a flowmeter prior to irradiation and monitored periodically during the reaction. [b] The percent conversion to hydroperoxide products is calculated using ^{1}H NMR peak areas, average and (standard deviation) reported for three experiments. All experiments were conducted on 0.3 M 2-methyl-2-butene in a benzene-d_6 solvent and irradiated at 420 nm for 1 h under an oxygen-rich environment.

(Scheme 1). As was observed by Shinohara et al., this reaction produces a ~1:1 ratio of the two hydroperoxide products 1 and 2. Each species possesses a well-resolved and unique hydrogen chemical shift (H_a, δ 4.93; H_b, δ 3.97; H_c, δ 5.50) in the ^{1}H NMR, corresponding to the area of one hydrogen and leading to the ready analysis of reaction mixtures using integration of ^{1}H NMR peak areas. The reaction time was optimized at 1 h to yield ~10 % conversion of starting material, thereby avoiding the appearance of side products resulting from the degradation of peroxide products.

Table 1 summarizes the solution photochemistry of $Sc_3N@I_h$-C_{80} relative to C_{60} fullerene for the photooxidation of 2-methyl-2-butene via in situ generated singlet oxygen. All reactions are conducted at a 0.3 M concentration of 2-methyl-2-butene using a catalytic amount of fullerene photosensitizer. In the absence of fullerene sensitizer, no detectable products were obtained. However, a significant conversion to hydroperoxide products was observed in the presence of either C_{60} or $Sc_3N@I_h$-C_{80}, and given the experimental error associated with our process, little difference between the two types of fullerene sensitizers could be detected. Reducing the photocatalyst by an order of magnitude resulted in a significant decrease in the production of hydroperoxide products. A similar effect was observed by reducing the oxygen purge rate. This is not surprising because the production of singlet-oxygen-generated products is expected to depend on the partial pressure of oxygen in the reaction environment (45).

Molar Extinction Coefficients. The molar extinction coefficients were determined in a toluene solvent for isomerically purified $Sc_3N@I_h$-C_{80} at 420 and 536 nm and are reported in Figure 3, along with C_{60} values for comparison. The wavelength of 420 nm is chosen to coincide with our photochemical lamp emission λ_{max}. The 536 nm value is an approximate λ_{max} of the C_{60} visible spectrum. Beer's law plots of prepared dilution series produced linear plots and good correlation values.

(a)

Fullerene	Molar extinction coeff. @ 420 nm	Molar extinction coeff. @ 536 nm
C_{60}	827	982
Sc_3-MNF	15,800	6,600

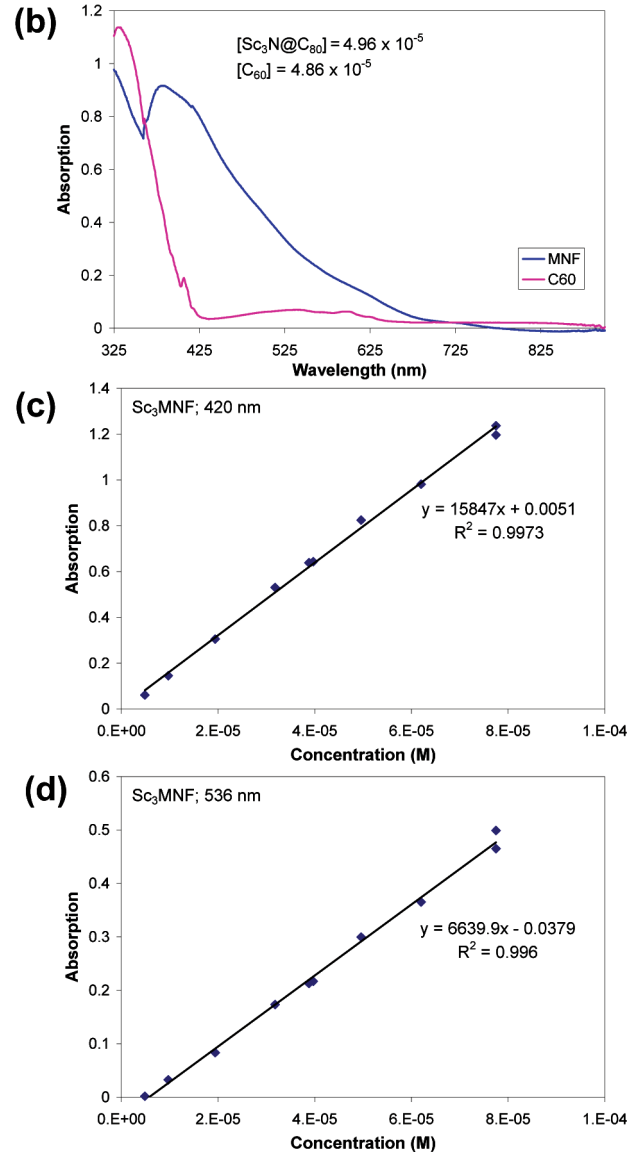

FIGURE 3. Determination of (a) molar absorptivity coefficients for isomerically purified $Sc_3N@I_h$-C_{80} at 420 and 536 nm using (b) UV/vis absorption spectra to generate (c and d) Beer's law plots.

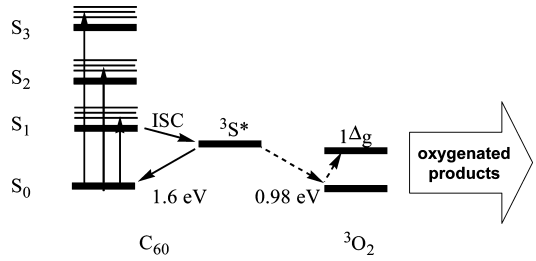

FIGURE 4. Energy level diagram for the interaction of excited-state C_{60} fullerene and ground-state molecular oxygen.

Several classical (non-MNF) EMFs have been investigated both as singlet-oxygen generators by Shinohara et al. (17) and as singlet-oxygen quenchers by Yanagi et al. (46). An example energy diagram, which describes the interaction between excited-state C_{60} fullerene and ground-state molecular oxygen, can be approximated by Figure 4. C_{60} is efficiently converted to the triplet excited state ($^3S^*$) upon UV irradiation, which efficiently sensitizes the formation of singlet oxygen ($^1O_2$) through an energy-transfer mechanism. Once generated, singlet oxygen is free to engage in additional molecular reactions. Shinohara et al. found that $Dy_2@C_{2n}$, $Dy@C_{82}$, and $Gd@C_{82}$ all successfully generated high yields of photooxidation products of 2-methyl-2-butene, while $La@C_{82}$ produced no reaction (17). This work was followed recently by Yanagi et al., who determined the total quenching rate constant (the sum of physical and chemical quenching mechanisms) for $La@C_{82}$ and several other fullerenes and found that $La@C_{82}$ possessed a quenching rate constant comparable to that of β-carotene (46). This process was discussed in terms of a combination of energy- and charge-transfer processes. The triplet state of the metallofullerene should lie slightly higher in energy than the $^1O_2$ energy for an efficient energy-transfer mechanism to occur. Our preliminary findings have significant data to support the generation of singlet oxygen from $Sc_3N@I_h$-C_{80}, tentatively placing a lower limit on the excited-state energy of $Sc_3N@I_h$-C_{80}. A continued investigation to measure more accurate rates and efficiencies for $^1O_2$ generation and probe potential quenching mechanisms and chemical reactivity considerations is ongoing.

Antimicrobial Studies. Films prepared using C_{60} and $Sc_3N@I_h$-C_{80} sensitizers were also evaluated for potential antimicrobial activity stemming from the in situ generation of $^1O_2$ under white light, and these results are summarized in Table 2. Techniques for biological assays were adapted from previously published reports (47, 48). Biological results for control samples—no sensitizer—afforded no biological activity against the two pathogenic bacteria examined in this study. A small additive effect was observed for fullerene-sensitized films, where C_{60} and $Sc_3N@I_h$-C_{80} provided a 1−2 log kill of both Gram-positive and Gram-negative bacteria. Multiple trials of each system were performed, and we suggest that C_{60} is a more active antimicrobial agent in these systems than $Sc_3N@I_h$-C_{80}. This finding is consistent with the photochemical film study, where tack measurements showed the generation of peroxide intermediates at a later time under identical conditions. Unfunctionalized fullerenes are hydrophobic and therefore insoluble in water, which prevents a direct comparison to solution antimicrobial studies. The ability of fullerenes to generate singlet oxygen is strongly influenced by chemical modification of the cage and other solubilizing procedures. However, a recent article by Markovic and Trajkovic (5) offers a current review of the photosensitization ability of select fullerenes, such as C_{60}, and their potential application as powerful antimicrobial agents.

Table 2. Antimicrobial Evaluation of Fullerene-Containing SIS Adhesive Films

sample ID	sensitizer concn (wt %)	film testing with *S. aureus*, Gram-positive[a]	film testing with *E. coli*, Gram-negative[a]
SIS control	none	0 log	0 log
SIS−C_{60}	0.2	1 log	2 log
SIS−C_{60}	1.0	2 log	2 log
SIS−$Sc_3N@I_h$-C_{80}	1.0	1 log	1 log

[a] Reported in log reduction from a starting concentration of 10^7 CFU/cm^2. Samples were performed in triplicate.

4. CONCLUSIONS

In conclusion, we have evaluated the singlet-oxygen-generating ability of $Sc_3N@I_h$-C_{80} in solution and SIS adhesive films. This work represents the first demonstration of the singlet-oxygen-generating ability of this family of compounds and the specific photochemical-sensitizing ability of $Sc_3N@I_h$-C_{80}. The rate of singlet-oxygen generation leading to oxidative cross-linking and subsequent loss of tack in adhesive films was slower for $Sc_3N@I_h$-C_{80} than for the classical fullerenes C_{60} and C_{70}, which had comparable rates. A reduced relative rate of singlet-oxygen production from $Sc_3N@I_h$-C_{80} is further supported by antimicrobial studies. However, in solution photochemical studies, where evidence for the production of singlet oxygen is supported by the successful photooxygenation of 2-methyl-2-butene to its allylic hydroperoxides, product yields suggested similar sensitization activity for $Sc_3N@I_h$-C_{80} and C_{60}.

Acknowledgment. J.P.P. thanks the NSF (Grant CHE-0847481) and the NIH (Grant R15AG028408; National Institute on Aging). Additional support from the Office of Naval Research (J.H.W.) and NSF (Grant CHE-0547988 to S.S.) is also acknowledged. Graduate Student Fellowships for M.A.M. (NSF GRFP) and C.E.C. (Department of Education, GAANN No. P200A060323) are also acknowledged.

REFERENCES AND NOTES

(1) Arbogast, J. W.; Darmanyan, A. P.; Foote, C. S.; Rubin, Y.; Diederich, F. N.; Alvarez, M. M.; Anz, S. J.; Whetten, R. L. *J. Phys. Chem.* **1991**, *95*, 11.
(2) Foote, C. S. *Top. Curr. Chem.* **1994**, *169*, 347.
(3) Guldi, D. M.; Asmus, K. D. *Radiat. Phys. Chem.* **1999**, *56*, 449.
(4) Guldi, D. M.; Prato, M. *Acc. Chem. Res.* **2000**, *33*, 695.
(5) Markovic, Z.; Trajkovic, V. *Biomaterials* **2008**, *29*, 3561.
(6) Nakamura, E.; Tokuyama, H.; Yamago, S.; Shiraki, T.; Sugiura, Y. *Bull. Chem. Soc. Jpn.* **1996**, *69*, 2143.
(7) Orfanopoulos, M.; Kambourakis, S. *Tetrahedron Lett.* **1995**, *36*, 435.
(8) Kai, Y.; Komazawa, Y.; Miyajima, A.; Miyata, N.; Yamakoshi, Y. *Fullerenes, Nanotubes, Carbon Nanostruct.* **2003**, *11*, 79.
(9) Bensasson, R. V.; Brettreich, M.; Frederiksen, J.; Gottinger, H.; Hirsch, A.; Land, E. J.; Leach, S.; McGarvey, D. J.; Schonberger, H. *Free Radical Biol. Med.* **2000**, *29*, 26.

(10) Bosi, S.; Da Ros, T.; Castellano, S.; Banfi, E.; Prato, M. *Bioorg. Med. Chem. Lett.* **2000**, *10*, 1043.
(11) Bosi, S.; Da Ros, T.; Spalluto, G.; Prato, M. *Eur. J. Med. Chem.* **2003**, *38*, 913.
(12) Bosi, S.; Feruglio, L.; Da Ros, T.; Spalluto, G.; Gregoretti, B.; Terdoslavich, M.; Decorti, G.; Passamonti, S.; Moro, S.; Prato, M. *J. Med. Chem.* **2004**, *47*, 6711.
(13) Da Ros, T.; Prato, M. *Chem. Commun.* **1999**, 663.
(14) Badireddy, A. R.; Hotze, E. M.; Chellam, S.; Alvarez, P.; Wiesner, M. R. *Environ. Sci. Technol.* **2007**, *41*, 6627.
(15) Tagmatarchis, N.; Shinohara, H. *Org. Lett.* **2000**, *2*, 3551.
(16) Tagmatarchis, N.; Shinohara, H.; Fujitsuka, M.; Ito, O. *J. Org. Chem.* **2001**, *66*, 8026.
(17) Tagmatarchis, N.; Okada, K.; Tomiyama, T.; Yoshida, T.; Kobayashi, Y.; Shinohara, H. *Chem. Commun.* **2001**, 1366.
(18) Alberti, M. N.; Orfanopoulos, M. *Tetrahedron* **2006**, *62*, 10660.
(19) Singleton, D. A.; Hang, C.; Szymanski, M. J.; Meyer, M. P.; Leach, A. G.; Kuwata, K. T.; Chen, J. S.; Greer, A.; Foote, C. S.; Houk, K. N. *J. Am. Chem. Soc.* **2003**, *125*, 1319.
(20) Stratakis, M.; Orfanopoulos, M. *Tetrahedron* **2000**, *56*, 1595.
(21) Tokuyama, H.; Nakamura, E. *J. Org. Chem.* **1994**, *59*, 1135.
(22) Chen, Z.; Fatouros, P. P.; Corwin, F. D.; Broaddus, W. C.; Dorn, H. C. *Neuro-Oncology* **2006**, *8*, 492.
(23) Fatouros, P. P.; Corwin, F. D.; Chen, Z. J.; Broaddus, W. C.; Tatum, J. L.; Kettenmann, B.; Ge, Z.; Gibson, H. W.; Russ, J. L.; Leonard, A. P.; Duchamp, J. C.; Dorn, H. C. *Radiology* **2006**, *240*, 756.
(24) Pinzon, J. R.; Plonska-Brzezinska, M. E.; Cardona, C. M.; Athans, A. J.; Gayathri, S. S.; Guldi, D. M.; Herranz, M. A.; Martin, N.; Torres, T.; Echegoyen, L. *Angew. Chem., Int. Ed.* **2008**, *47*, 4173.
(25) Fang, J. S.; Lyon, D. Y.; Wiesner, M. R.; Dong, J. P.; Alvarez, P. J. J. *Environ. Sci. Technol.* **2007**, *41*, 2636.
(26) Lyon, D. Y.; Adams, L. K.; Falkner, J. C.; Alvarez, P. J. J. *Environ. Sci. Technol.* **2006**, *40*, 4360.
(27) Lyon, D. Y.; Brunet, L.; Hinkal, G. W.; Wiesner, M. R.; Alvarez, P. J. J. *Nano Lett.* **2008**, *8*, 1539.
(28) Lyon, D. Y.; Fortner, J. D.; Sayes, C. M.; Colvin, V. L.; Hughes, J. B. *Environ. Toxicol. Chem.* **2005**, *24*, 2757.
(29) Li, Q. L.; Mahendra, S.; Lyon, D. Y.; Brunet, L.; Liga, M. V.; Li, D.; Alvarez, P. J. J. *Water Res.* **2008**, *42*, 4591.
(30) Barber, R. P.; Gomez, R. D.; Herman, W. N.; Romero, D. B. *Org. Electron.* **2006**, *7*, 508.
(31) Dennler, G.; Lungenschmied, C.; Neugebauer, H.; Sariciftci, N. S.; Latreche, M.; Czeremuszkin, G.; Wertheimer, M. R. *Thin Solid Films* **2006**, *511*, 349.
(32) Janssen, R. A. J.; Hummelen, J. C.; Saricifti, N. S. *MRS Bull.* **2005**, *30*, 33.
(33) Antipov, O. L.; Yurasova, I. V.; Domrachev, G. A. *Quantum Electron.* **2002**, *32*, 776.
(34) Elim, H. I.; Ji, W.; Meng, G. C. *J. Nonlinear Opt. Phys. Mater.* **2003**, *12*, 175.
(35) Kamanina, N. V. *Synth. Met.* **2003**, *139*, 547.
(36) Zeng, H. P.; Sun, Z. R.; Segawa, Y.; Lin, F. C.; Mao, S.; Xu, Z. Z. *J. Appl. Phys.* **2001**, *89*, 6539.
(37) Amao, Y. *Microchim.Acta* **2003**, *143*, 1.
(38) Phillips, J. P.; Deng, X.; Stephen, R. R.; Fortenberry, E. L.; Todd, M. L.; McCluskey, D. M.; Stevenson, S.; Misra, R.; Morgan, S. E.; Long, T. E. *Polymer* **2007**, *48*, 6773.
(39) Phillips, J. P.; Deng, X.; Todd, M. L.; Heaps, D. T.; Stevenson, S.; Zhou, H.; Hoyle, C. E. *J. Appl. Polym. Sci.* **2008**, *109*, 2895.
(40) Satas, D. *Handbook of Pressure Sensitive Adhesive Technology*; Status & Associates: Warwick, RI, 1999.
(41) Florian, S.; Novak, I. *J. Mater. Sci.* **2004**, *39*, 649.
(42) Sung, I. K.; Kim, K. S.; Chin, I. J. *Polym. J.* **1998**, *30*, 181.
(43) Stevenson, S.; Harich, K.; Yu, H.; Stephen, R. R.; Heaps, D.; Coumbe, C.; Phillips, J. P. *J. Am. Chem. Soc.* **2006**, *128*, 8829.
(44) Stevenson, S.; Thompson, M. C.; Coumbe, H. L.; Mackey, M. A.; Coumbe, C. E.; Phillips, J. P. *J. Am. Chem. Soc.* **2007**, *129*, 16257.
(45) Arai, H.; Tajima, Y.; Takeuchi, K. *Jpn J. Appl. Phys., Part 1* **2001**, *40*, 6623.
(46) Yanagi, K.; Okubo, S.; Okazaki, T.; Kataura, H. *Chem. Phys. Lett.* **2007**, *435*, 306.
(47) Pant, R. R.; Buckley, J. L.; Fulmer, P. A.; Wynne, J. H.; McCluskey, D. M.; Phillips, J. P. *J. Appl. Polym. Sci.* **2008**, *110*, 3080.
(48) Wynne, J. H.; Pant, R. R.; Jones-Meehan, J. M.; Phillips, J. P. *J. Appl. Polym. Sci.* **2008**, *107*, 2089.

AM900008V